

Antibacterial and cytotoxic metabolites produced by *Streptomyces tanashiensis* BYF-112 isolated from *Odontotermes formosanus*

Jun WU, Tao SONG, Le ZHANG, Zhongdi HUANG, Fang HUANG, Caiping YIN, Shuxiang ZHANG, Xinhua LIU, Yinglao ZHANG

**Citation:** Jun WU, Tao SONG, Le ZHANG, Zhongdi HUANG, Fang HUANG, Caiping YIN, Shuxiang ZHANG, Xinhua LIU, Yinglao ZHANG, Antibacterial and cytotoxic metabolites produced by *Streptomyces tanashiensis* BYF-112 isolated from *Odontotermes formosanus*, *Chinese Journal of Natural Medicines*, 2024, 22(9), 822–830. doi: [10.1016/S1875-5364\(24\)60720-X](https://doi.org/10.1016/S1875-5364(24)60720-X).

View online: [https://doi.org/10.1016/S1875-5364\(24\)60720-X](https://doi.org/10.1016/S1875-5364(24)60720-X)

## Related articles that may interest you

The antibacterial activity of *Berberis heteropoda* Schrenk and its effect on irritable bowel syndrome in rats

*Chinese Journal of Natural Medicines*. 2020, 18(5), 356–368 [https://doi.org/10.1016/S1875-5364\(20\)30042-X](https://doi.org/10.1016/S1875-5364(20)30042-X)

A comprehensive review of natural products with anti-hypoxic activity

*Chinese Journal of Natural Medicines*. 2023, 21(7), 499–515 [https://doi.org/10.1016/S1875-5364\(23\)60410-8](https://doi.org/10.1016/S1875-5364(23)60410-8)

New meroterpenoid compounds from the culture of mushroom *Panus lecomtei*

*Chinese Journal of Natural Medicines*. 2020, 18(4), 268–272 [https://doi.org/10.1016/S1875-5364\(20\)30033-9](https://doi.org/10.1016/S1875-5364(20)30033-9)

Lysohexaenitides A and B, linear lipopeptides from *Lysobacter* sp. DSM 3655 identified by heterologous expression in *Streptomyces*

*Chinese Journal of Natural Medicines*. 2023, 21(6), 454–458 [https://doi.org/10.1016/S1875-5364\(23\)60473-X](https://doi.org/10.1016/S1875-5364(23)60473-X)

Recent progress on anti-*Candida* natural products

*Chinese Journal of Natural Medicines*. 2021, 19(8), 561–579 [https://doi.org/10.1016/S1875-5364\(21\)60057-2](https://doi.org/10.1016/S1875-5364(21)60057-2)

Advances in the role of natural products in human gene expression

*Chinese Journal of Natural Medicines*. 2022, 20(1), 1–8 [https://doi.org/10.1016/S1875-5364\(22\)60147-X](https://doi.org/10.1016/S1875-5364(22)60147-X)



Wechat

•Original article•

## Antibacterial and cytotoxic metabolites produced by *Streptomyces tanashiensis* BYF-112 isolated from *Odontotermes formosanus*

WU Jun<sup>1</sup>, SONG Tao<sup>1</sup>, ZHANG Le<sup>1</sup>, HUANG Zhongdi<sup>1</sup>, HUANG Fang<sup>1</sup>, YIN Caiping<sup>1</sup>,  
ZHANG Shuxiang<sup>1</sup>, LIU Xinhua<sup>2</sup>, ZHANG Yinglao<sup>1\*</sup>

<sup>1</sup> School of Life Science, Anhui Agricultural University, Hefei 230036, China;

<sup>2</sup> School of Pharmacy, Anhui Medical University, Hefei 230036, China

Available online 20 Sep., 2024

**[ABSTRACT]** Chemical investigations of the termite-associated *Streptomyces tanashiensis* BYF-112 resulted in the discovery of four novel alkaloid derivatives: vegfrecines A and B (**1** and **2**), exfoliazone A (**3**), and venezueline H (**7**), in addition to nine known metabolites (**4–6**, **8–13**). The structures of these compounds were elucidated through comprehensive spectroscopic analysis and comparison with existing literature data. Antibacterial assays revealed that viridomycin A (**11**) exhibited potent antibacterial activity against *Staphylococcus aureus*, with a zone of inhibition (ZOI) of 12.67 mm, in comparison to a ZOI of 17.67 mm for the positive control gentamicin sulfate. Viridomycin A (**11**) showed moderate activity against *Micrococcus tetragenus* and *Pseudomonas syringae* pv. *actinidae*, with ZOI values of 15.50 and 14.33 mm, respectively, which were inferior to those of gentamicin sulfate (34.67 and 24.00 mm). Viridomycin F (**12**) also exhibited moderate antibacterial effects against *S. aureus*, *M. tetragenus*, and *P. syringae* pv. *actinidae*, with ZOI values of 8.33, 16.50, and 10.83 mm, respectively. Cytotoxicity assays demonstrated that viridobruunine A (**5**), exfoliazone (**6**), viridomycin A (**11**), and X-14881E (**13**) exhibited significant cytotoxicity against human malignant melanoma (A375), ovarian cancer (SKOV-3), and gastric cancer (MGC-803) cell lines, with IC<sub>50</sub> values ranging from 4.61 to 19.28 μmol·L<sup>-1</sup>. Furthermore, bioinformatic analysis of the complete genome of *S. tanashiensis* suggested a putative biosynthetic gene cluster (BGC) responsible for the production of compounds **1–12**. These findings indicate that the secondary metabolites of insect-associated *S. tanashiensis* BYF-112 hold promise as potential sources of novel antibacterial and anticancer agents.

**[KEY WORDS]** *Odontotermes formosanus*; *Streptomyces tanashiensis*; Alkaloid; Cytotoxic activity; Antibacterial activity; Biosynthetic pathway

**[CLC Number]** R284.1, R965    **[Document code]** A    **[Article ID]** 2095-6975(2024)09-0822-09

### Introduction

Despite extensive research into microbial natural products from *Streptomyces* species, there remains significant untapped potential within this genus, particularly those inhabiting unique ecological niches [1]. Insects often thrive in specialized habitats due to their associations with microbial symbionts [2]. Recent research estimates the total number of living insect species at 5.5 million [3], with at least 15%–20% of these insects engaged in symbiotic relationships with mi-

crobes [4]. The vast diversity of insect species hosting extensive symbiotic microbial communities represents a substantial resource for discovering novel bioactive natural products [5–8]. For example, amycolamycin A, a novel enediyne-derived natural product from a locust-associated *Amycolatopsis* sp. HC4, demonstrated selective cytotoxicity against the M231 breast cancer cell line [9]. Similarly, fasamycins D and E, novel pentacyclic polyketides isolated from *Streptomyces formicae* associated with African *Tetraponera* plant-ants, showed significant antibacterial activity against *Bacillus subtilis*, methicillin-resistant *Staphylococcus aureus*, and vancomycin-resistant *Enterococcus faecium* [10]. However, to our knowledge, there have been few studies focusing on the bioactive compounds from insect symbionts.

In our ongoing efforts to discover novel bioactive microbial metabolites from insect-derived microorganisms [11, 12], we identified *Streptomyces tanashiensis* BYF-112, isolated from *Odontotermes formosanus*, which exhibited potent anti-

**[Received on]** 07-Nov.-2023

**[Research funding]** This work was supported by the Natural Science Funds for Distinguished Young Scholars of Anhui Province (No. 2108085J18) and the National Natural Science Foundation of China (Nos. 32011540382 and 32102272).

**[\*Corresponding author]** Tel: 86-551-6578-6129, E-mail: [zhangyl@ahau.edu.cn](mailto:zhangyl@ahau.edu.cn)

These authors have no conflict of interest to declare.

bacterial and cytotoxic activities [13]. Bioactivity-guided fractionation of the crude extract led to the discovery of four new alkaloid derivatives: vegfrecines A and B (**1** and **2**), exfoliazone A (**3**), and venezueline H (**7**), along with nine known metabolites (**4–6**, **8–13**) (Fig. 1). Herein, we report the detailed isolation, chemical characterization, and bioactivity (cytotoxic and antibacterial) of compounds **1–13**. Additionally, we propose the possible biosynthetic pathways for compounds **1–12** based on genetic analysis.

## Results and Discussion

Vegfrecine A (**1**) was isolated as a magenta solid. Its molecular formula,  $C_{15}H_{12}N_2O_5$ , was determined by HR-ESI-MS, showing an ion peak at  $(m/z [M + Na]^+ 323.0641$ , Calcd. for  $C_{15}H_{12}N_2O_5Na 323.0642$ ). This result was consistent with the  $^1H$  and  $^{13}C$  NMR data (Table 1 and Figs. S2–S8). The  $^1H$  NMR spectrum of **1** displayed signals for an aldehyde group at  $\delta_H$  9.82 (s, 1H) and two amino groups at  $\delta_H$  9.73 (s, 1H) and 8.84 (s, 1H). The  $^{13}C$  NMR and DEPT135 spectra showed signals for four carbonyl carbons ( $\delta_C$  190.7, 183.5, 179.6, and 171.3), ten olefinic carbons ( $\delta_C$  97.2, 109.4, 116.4, 124.7, 125.6, 128.1, 129.1, 141.6, 144.2, and 157.0), and one methyl carbon ( $\delta_C$  24.5). The heteronuclear multiple bond correlations (HMBC) spectrum of **1** showed correlations (Fig. 2) from H-1 ( $\delta_H$  7.34) to C-2 ( $\delta_C$  141.6), C-3 ( $\delta_C$  179.6), and C-5 ( $\delta_C$  144.2), from H-4 ( $\delta_H$  5.64) to C-2 and C-6 ( $\delta_C$  183.5), and from -NH ( $\delta_H$  9.73) to C-1, C-3 and C-7 ( $\delta_C$  171.3), indicating the presence of an *N*-(3,6-dioxocyclohexa-1,4-dien-1-yl) acetamide moiety. Further analysis of the HMBC data showed correlations from H-3' ( $\delta_H$  7.08) to C-1' ( $\delta_C$  125.6) and C-5' ( $\delta_C$  128.1), from H-4' ( $\delta_H$  7.67) to C-2' ( $\delta_C$  157.0) and C-6' ( $\delta_C$  124.7), from H-6' ( $\delta_H$  7.77) to C-2', C-4' ( $\delta_C$  129.1) and C-7' ( $\delta_C$  190.7), and from H-7' ( $\delta_H$  9.82) to C-4' and C-6'. Additionally,  $^1H$ - $^1H$ -correlation spectroscopy (COSY) correlations (Fig. 2) between H-3' and H-4' confirmed the presence of a 4-hydroxybenzaldehyde moiety. The attachment of the 1'-NH group to the C-5 position was established by HMBs from 1'-NH ( $\delta_H$  8.84) to C-4 and C-6'. These data closely matched those of vegfrecine, an inhibitor of VEGF receptor tyrosine kinases first isolated from the culture broth of *Streptomyces* sp. MK931-CF8 [14]. Accordingly, the structure of **1** was established as a new vegfrecine derivative, and the name vegfrecine A was proposed for this compound.

Vegfrecine B (**2**) was isolated as a magenta solid. Its molecular formula,  $C_{15}H_{14}N_2O_5$ , was determined by HR-ESI-MS, which showed ion peaks at  $m/z$  303.0978  $[M + H]^+$  and 325.0975  $[M + Na]^+$ . These values were consistent with  $^1H$  and  $^{13}C$  NMR data (Table 2 and Figs. S11–S117). The comparison of the NMR data of vegfrecine B (**2**) with those of vegfrecine A (**1**) indicated that both compounds share the same core structure. The significant difference between the two compounds was the substitution of the aldehyde group at C-7' ( $\delta_H$  9.82,  $\delta_C$  190.7) in compound **1** with an oxygenated methylene group at C-7' ( $\delta_H$  4.58,  $\delta_C$  63.9) in compound **2**.

**Table 1**  $^1H$  (600 MHz) and  $^{13}C$  (150 MHz) NMR for vegfrecines A–B (**1** and **2**)

No.	1 <sup>a</sup>		2 <sup>b</sup>	
	$\delta_C$ , type	$\delta_H$ , mult (J in Hz)	$\delta_C$ , type	$\delta_H$ , mult (J in Hz)
1	109.4, CH	7.34, s	109.9, CH	7.41, s
2	141.6, C		142.3, C	
3	179.6, C		180.5, C	
4	97.2, CH	5.64, s	97.4, CH	5.93, s
5	144.2, C		144.8, C	
6	183.5, C		184.4, C	
7	171.3, C		170.9, C	
8	24.5, CH <sub>3</sub>	2.22, s	24.6, CH <sub>3</sub>	2.30, s
1'	125.6, C		125.7, C	
2'	157.0, C		149.2, C	
3'	116.4, CH	7.08, d (8.3)	116.3, CH	6.99, d (8.2)
4'	129.1, CH	7.67, dd (8.4, 1.9)	125.5, CH	7.08, d (8.2)
5'	128.1, C		135.5, C	
6'	124.7, CH	7.77, d (1.9)	121.4, CH	7.41, s
7'	190.7, C	9.82, s	63.9, CH <sub>2</sub>	4.58, s
2'-OH				
7'-OH				5.91, br s
2-NH		9.73, br s		9.05, br s
5-NH		8.84, br s		8.33, br s

<sup>a</sup> Recorded in DMSO- $d_6$ ; <sup>b</sup> Recorded in acetone- $d_6$ .

This substitution was confirmed by HMBs (Fig. 2) from H-7' ( $\delta_H$  4.58) to C-4' ( $\delta_C$  125.5) and C-6' ( $\delta_C$  121.4), from H-4' ( $\delta_H$  7.08) to C-7' ( $\delta_C$  63.6), and from H-6' ( $\delta_H$  7.41) to C-7'. Based on these findings, the structure of vegfrecine B (**2**) was established as a new derivative of vegfrecine, and it was given the trivial name vegfrecine B.

Exfoliazone A (**3**) was isolated as a red solid. Its molecular formula,  $C_{14}H_{12}N_2O_3$ , was determined by HR-ESI-MS, which showed an ion peak at  $m/z [M + H]^+ 257.0930$  (calculated for  $C_{14}H_{13}N_2O_3$ ). This result was consistent with the  $^1H$  and  $^{13}C$  NMR data (Table 2 and Fig. S18–S24). The  $^1H$  NMR spectrum of **3** exhibited a hydroxyl signal at  $\delta_H$  5.31 (t,  $J = 5.8$  Hz, 1H) and an amino group signal at  $\delta_H$  7.14 (brs, 1H).  $^{13}C$  NMR and DEPT135 spectra displayed signals for one carbonyl carbon ( $\delta_C$  179.6), five olefinic carbons ( $\delta_C$  149.4, 147.9, 146.9, 103.2, and 95.1), six tri-substituted aromatic ring carbons ( $\delta_C$  140.6, 139.9, 133.4, 126.9, 125.2, and 115.5), one methylene carbon ( $\delta_C$  62.1) and one methyl carbon ( $\delta_C$  28.9). The HMBC spectrum of **3** showed correlations from H-1 ( $\delta_H$  6.36) to C-3 ( $\delta_C$  146.9) and C-5 ( $\delta_C$  147.9), from H-4 ( $\delta_H$  6.11) to C-2 ( $\delta_C$  179.6) and C-6 ( $\delta_C$  149.4), and from H-1' ( $\delta_H$  2.86) to C-3, together with  $^1H$ - $^1H$ -COSY correlations (Fig. 2) observed between H-1' and -NH,

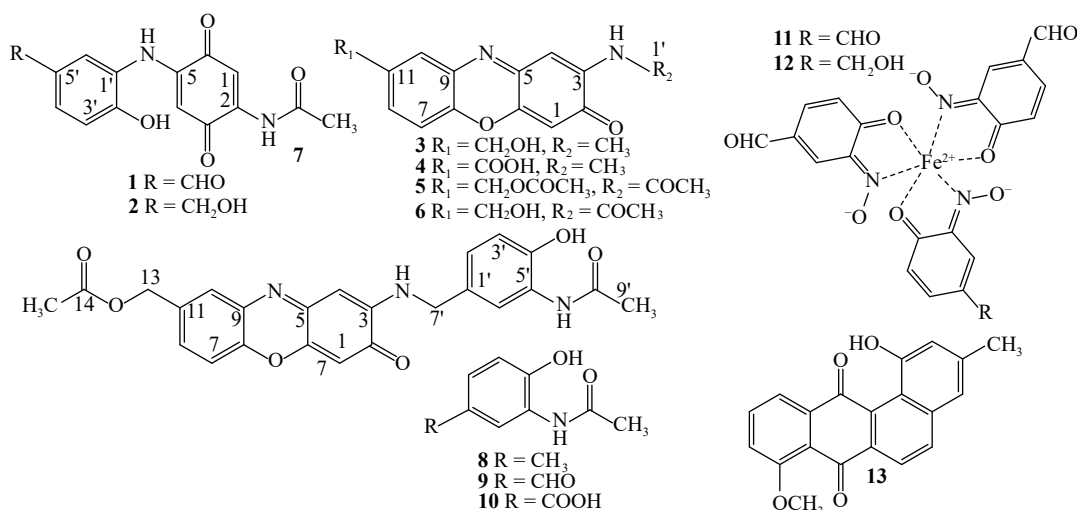


Fig. 1 Chemical structures of secondary metabolites 1–13 of *Streptomyces tanashiensis* BYF-112.

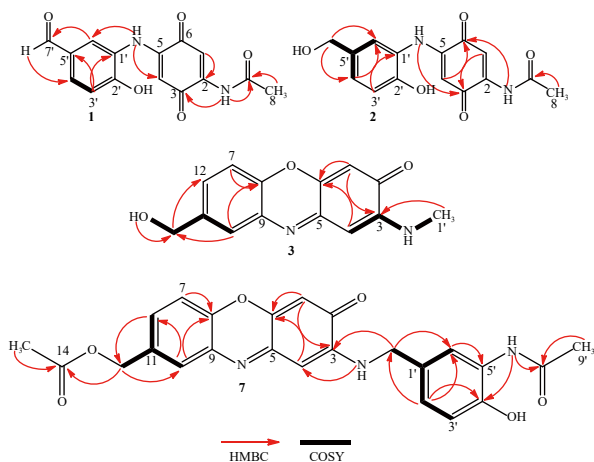


Fig. 2 Key HMBCs (red arrows) and key <sup>1</sup>H–<sup>1</sup>H COSY (black bold lines) of vegfrecines A–B (**1** and **2**), exfoliazone A (**3**), and venezueline H (**7**).

revealing the presence of a 2-(methylamino)cyclohexa-2,5-dien-1-one unit. Further analysis of the HMBC data showed correlations from H-7 ( $\delta_{\text{H}}$  7.46) to C-9 ( $\delta_{\text{C}}$  133.4), and C-11 ( $\delta_{\text{C}}$  139.9), from H-10 ( $\delta_{\text{H}}$  7.63) to C-13 ( $\delta_{\text{C}}$  62.1), C-18 ( $\delta_{\text{C}}$  140.6), and C-12 ( $\delta_{\text{C}}$  126.9), from H-12 ( $\delta_{\text{H}}$  7.40) to C-8 ( $\delta_{\text{C}}$  140.6), C-10 and C-13, from H-13 ( $\delta_{\text{H}}$  4.59) to C-10, C-11, and C-12, and from H-O ( $\delta_{\text{H}}$  5.31) to C-11 and C-13, indicating the presence of a phenylmethanol moiety. The data for exfoliazone A (**3**) were nearly identical to those of exfoliazone, a natural product first isolated from the culture broth of *Streptomyces exfoliatus* BT-38 [15]. Accordingly, the structure of **3** was established as a new exfoliazone derivative, and the name exfoliazone A was proposed for this compound.

Exfoliazone (**6**) and venezueline H (**7**) were isolated as a 1 : 1 mixture. A detailed comparison of the NMR data for this mixture (**6** and **7**) with those of compound **3** (Figs. S30–S35) revealed structural similarities. The major differences included CH<sub>2</sub>-13 ( $\delta_{\text{H}}$  4.59, d;  $\delta_{\text{C}}$  62.1) and CH<sub>3</sub>-1' ( $\delta_{\text{H}}$  2.86, d;  $\delta_{\text{C}}$  28.9) in compound **3** (Table 3) being replaced by

Table 2 <sup>1</sup>H (600 MHz) and <sup>13</sup>C (150 MHz) NMR for exfoliazone A (**3**) in DMSO-*d*<sub>6</sub>

No.	$\delta_{\text{C}}$ , type	$\delta_{\text{H}}$ , mult (J in Hz)
1	103.1, CH	6.36, s
2	179.6, C	
3	146.9, C	
4	95.1, CH	6.11, s
5	147.9, C	
6	149.4, C	
7	115.5, CH	7.46, d (8.4)
8	140.6, C	
9	133.4, C	
10	125.2, CH	7.63, s
11	139.9, C	
12	126.9, CH	7.40, dd (8.4, 1.8)
13	62.1, CH <sub>2</sub>	4.59, d (5.6)
1'	28.9, CH <sub>3</sub>	2.86, d (5.2)
-OH		5.31, t (5.8)
-NH		7.14, br s

CH<sub>2</sub>-13 ( $\delta_{\text{H}}$  5.14, s;  $\delta_{\text{C}}$  64.6) and CH<sub>2</sub>-7' ( $\delta_{\text{H}}$  4.35, d;  $\delta_{\text{C}}$  45.2) in compound **7**, and C-1' ( $\delta_{\text{C}}$  170.6) in compound **6**. The monomer of **6** was subsequently isolated, and its <sup>1</sup>H, <sup>13</sup>C NMR, and HR-ESI-MS data revealed a known phenoxazinone (Figs. S27–S29) [15], consistent with the proposed structure. Excluding the NMR data of compound **6**, the remaining NMR signals indicated the presence of an acetyl group ( $\delta_{\text{C}}$  64.6, 170.2, 23.5) and a 3'-*N*-acetyl-4'-hydroxyphenyl group ( $\delta_{\text{C}}$  128.3, 23.6, 135.9, 147.0, 126.4, 121.1, 169.0, 20.7) in compound **7**. The HMBC spectrum provided further structural details for compound **7**. Correla-

**Table 3**  $^1\text{H}$  (600 MHz) and  $^{13}\text{C}$  (150 MHz) NMR for Venezueline H (**7**) in DMSO- $d_6$ 

No.	$\delta_{\text{C}}$ , type	$\delta_{\text{H}}$ , mult (J in Hz)
1	103.5, CH	6.39 s
2	179.9, C	
3	145.7, C	
4	96.2, CH	6.05 s
5	148.0, C	
6	149.2, C	
7	116.0, CH	7.49, d (8.3)
8	141.5, C	
9	133.2, C	
10	127.0, CH	7.65, s
11	133.4, C	
12	128.4, CH	7.44, dd (8.3, 1.8)
13	64.6, CH <sub>2</sub>	5.14, s
14	170.2, C	
15	23.5, CH <sub>3</sub>	2.08, s
1'	128.3, C	
2'	121.1, CH	7.68, s
3'	126.4, C	
4'	147.0, C	
5'	115.9, CH	6.82, d (8.1)
6'	123.6, CH	6.97, d (8.1)
7'	45.2, CH <sub>2</sub>	4.36, d (6.3)
8'	169.0, C	
9'	20.7, CH <sub>3</sub>	2.08, s
4'-OH		9.31, br s
3-NH		7.65, br s
3'-NH		9.31, br s

tions from H-13 ( $\delta_{\text{H}}$  5.14) to C-10 ( $\delta_{\text{C}}$  127.0), C-11 ( $\delta_{\text{C}}$  133.4), C-12 ( $\delta_{\text{C}}$  128.8) and C-14 ( $\delta_{\text{C}}$  170.2) indicated an aldehyde group at position 13. Additionally, correlations from H-7' ( $\delta_{\text{H}}$  4.36) to C-3 ( $\delta_{\text{C}}$  145.7), C-2' ( $\delta_{\text{C}}$  121.1), and C-6' ( $\delta_{\text{C}}$  123.6) indicated a 3'-*N*-acetyl-4'-hydroxyphenyl group at 7'. The HR-ESI-MS data ( $m/z$  470.1320 [ $\text{M} + \text{Na}$ ]<sup>+</sup>, 486.1077 [ $\text{M} + \text{K}$ ]<sup>+</sup>) further confirmed this structure (Fig. S37). Based on these data, the structure of compound **7** was established as a new venezueline derivative, named venezueline H.

The other secondary metabolites were identified as texazone (**4**)<sup>[16]</sup>, viridobruanine A (**5**)<sup>[17]</sup>, *N*-(2-Hydroxy-5-methylphenyl) acetamide (**8**)<sup>[18]</sup>, 3-acetyl-amino-4-hydroxybenzaldehyde (**9**)<sup>[19]</sup>, 3-acetamido-4-hydroxybenzoic acid (**10**)<sup>[20]</sup>, viridomycin A (**11**)<sup>[21]</sup>, viridomycin F (**12**)<sup>[21]</sup>, and X-14881E (**13**)<sup>[22]</sup> by spectroscopic data analysis and comparis-

on with literature data (Fig. 1).

*Streptomyces tanashiensis* is renowned for producing a diverse array of secondary metabolites with significant biological activities. Previous research has led to the isolation of several bioactive compounds, including the antitumor antibiotics leptofuranins A–D<sup>[23]</sup>, the antibiotic tetrahydrokalamfungin<sup>[24]</sup>, the antibiotic lactoquinomycin A and B<sup>[25,26]</sup>, and the antimicrobial agent kalafungin<sup>[27]</sup>. However, this study marks the first report of new alkaloids (**1–3**, **7**) and the metabolites (**4–6**, **8–13**) produced by *S. tanashiensis* BYF-112, which was isolated from the surface of *Odontotermes formosanus*.

#### Antibacterial assay

The antibacterial activities of the isolated metabolites (except for compounds **2** and **7**) were evaluated against two gram-positive bacteria (*Staphylococcus aureus* and *M. tetragenus*) and two gram-negative bacteria (*P. syringae* pv. *actinidae* and *E. coli*). The results (Table 4) indicate that viridomycin A (**11**) exhibited strong antibacterial activity against *S. aureus*, with a zone of inhibition (ZOI) of 12.67 mm, which is comparable to the ZOI of 17.67 mm observed for gentamicin sulfate. Exfoliazone (**6**) and viridomycin F (**12**) displayed moderate antibacterial effects against *S. aureus*, with ZOI values of 6.83 and 8.33 mm, respectively. Moreover, viridomycin A (**11**), viridomycin F (**12**), and X-14881E (**13**) showed moderate antibacterial activity against *M. tetragenus*, with the ZOI values of 15.50, 16.50, and 11.67 mm, respectively, compared to the ZOI of 34.67 mm for gentamicin sulfate. Exfoliazone A (**3**), viridomycin A (**11**), and viridomycin F (**12**) also demonstrated moderate antibacterial effects against *P. syringae* pv. *actinidae* with ZOI

**Table 4** Inhibitory effects of **1**, **3–6**, and **8–13** against four pathogenic bacteria (mean  $\pm$  SD,  $n = 3$ )

Compounds	ZOI (mm) <sup>a</sup>			
	<i>S. aureus</i>	<i>M. tetragenus</i>	Psa <sup>b</sup>	<i>E. coli</i>
<b>1</b>	NI <sup>c</sup>	NI	NI	NI
<b>3</b>	NI	NI	10.33 $\pm$ 1.15	NI
<b>4</b>	NI	NI	NI	NI
<b>5</b>	NI	NI	NI	NI
<b>6</b>	6.83 $\pm$ 0.76	NI	NI	NI
<b>8</b>	NI	NI	NI	NI
<b>9</b>	NI	NI	NI	NI
<b>10</b>	NI	NI	NI	NI
<b>11</b>	12.67 $\pm$ 0.58	15.50 $\pm$ 0.87	14.33 $\pm$ 0.58	NI
<b>12</b>	8.33 $\pm$ 0.58	16.50 $\pm$ 0.87	10.83 $\pm$ 0.29	NI
<b>13</b>	NI	11.67 $\pm$ 0.58	NI	NI
Gentamicin sulfate <sup>d</sup>	17.67 $\pm$ 0.58	34.67 $\pm$ 0.58	24.00 $\pm$ 1.00	22.67 $\pm$ 0.58

<sup>a</sup>ZOI: zone of inhibition; <sup>b</sup>Psa: *Pseudomonas syringae* pv. *actinidae*;

<sup>c</sup>NI: not inhibited, 30  $\mu\text{g}/\text{disc}$ ; <sup>d</sup>Gentamicin sulfate: positive control.

values of 10.33, 14.33, and 10.83 mm, respectively, compared to a ZOI of 24.00 mm for gentamicin sulfate. Unfortunately, all compounds were inactive against *E. coli*.

Questionmycin A, a phenoxazinone without additional substitutions at C-3 and C-11, has been reported to exhibit potent antibacterial activity against both gram-positive and gram-negative bacteria [28]. Our results suggest that phenoxazinones with additional substitutions at C-3 and C-11 show reduced or no antibacterial activity against pathogenic bacteria. This implies that *S. tanashiensis* BYF-112 might produce enzymes that chemically modify these toxic products, thereby reducing their toxicity and accumulation within the cells.

#### Cytotoxicity assay

The cytotoxicity of the metabolites (**1–6**, **8–11**, and **13**) was evaluated against various cancer cell lines, including A375 (melanoma), SKOV-3 (ovarian cancer), MDA-MB-231 (breast cancer), and MGC-803 (gastric cancer), as well as the normal cell line L20 (Table 5). The results showed that viridobruunine A (**5**), exfoliazone (**6**), viridomycin A (**11**), and X-14881E (**13**) exhibited significant cytotoxicity against A375, SKOV-3, and MGC-803, with IC<sub>50</sub> values ranging from 4.61 to 19.28 μmol·L<sup>-1</sup>. Unfortunately, viridobruunine A (**5**), exfoliazone (**6**), and X-14881E (**13**) also exhibited cytotoxic activities to also showed cytotoxicity against the normal cell line L02, with IC<sub>50</sub> values ranging from 56.41 to 79.68 μmol·L<sup>-1</sup>. Notably, viridomycin A (**11**) did not exhibit cytotoxicity against the normal cell line L20 (IC<sub>50</sub> > 100 μmol·L<sup>-1</sup>), indicating its potential as a lead compound for anticancer therapy. Among the other tested compounds, the novel metabolite **1** showed weak cytotoxicity against SKOV-3 with an IC<sub>50</sub> value of 76.18 μmol·L<sup>-1</sup>, while the novel com-

ound **2** displayed moderate cytotoxicity against A375, with an IC<sub>50</sub> value of 47.25 μmol·L<sup>-1</sup>. Additionally, 3-acetamido-4-hydroxybenzoic acid (**10**) demonstrated moderate cytotoxicity against A375 (IC<sub>50</sub> 22.01 μmol·L<sup>-1</sup>) and MGC-803 (IC<sub>50</sub> 36.29 μmol·L<sup>-1</sup>). It is noteworthy that among compounds **3–6**, which share a similar skeleton, only viridobruunine A (**5**) and exfoliazone (**6**) showed significant cytotoxicity. This suggests that the presence of an *N*-acetyl group at the C-3 position in phenoxazinones may enhance their cytotoxicity.

#### Proposed biosynthetic pathway of compounds 1–12

Previous studies have suggested that compounds **3–12** are derived from the precursor 3-amino-4-hydroxybenzoic acid (3,4-AHBA) [20, 29]. Specifically, *N*-(2-Hydroxy-5-methylphenyl) acetamide (**8**), 3-acetyl-amino-4-hydroxybenzaldehyde (**9**), and 3-acetamido-4-hydroxybenzoic acid (**10**) are known derivatives of 3,4-AHBA. Additionally, the newly identified alkaloids vegfrecine A (**1**) and vegfrecine B (**2**) feature a unique *p*-benzoquinone ring with amino and carboxamide groups, similar to those in 3,4-AHBA. This suggests that compounds **1–12** might be produced via a shared biosynthetic pathway. To elucidate the BGCs responsible for the production of compounds **1–12** in *S. tanashiensis* BYF-112, the genome was analyzed using antiSMASH v6.0.1, with a focus on identifying the 3,4-AHBA synthase. The analysis revealed one candidate cluster, BGC10, which is similar to the grixazone BGC found in *S. griseus* [30]. This cluster is likely responsible for the biosynthesis of compounds **1–12** (Table S1). Comparative analysis with the grixazone cluster identified thirteen homologous genes in BGC10, including those encoding aspartokinase, DhnA-type aldolase, 3,4-AHBA synthase, 3,4-AHBA transporter, *o*-aminophenol oxidase, cop-

**Table 5** Cytotoxic effects of compounds **1–6**, **8–11** and **13** against A375, SKOV-3, MDA-MB-231, MGC-803, and L02 cells (mean ± SD, *n* = 3)

Compounds	IC <sub>50</sub> (μmol·L <sup>-1</sup> ) <sup>a</sup>				
	A375	SKOV-3	MDA-MB-231	MGC-803	L02
<b>1</b>	> 100	76.18 ± 2.09	> 100	> 100	> 100
<b>2</b>	47.25 ± 0.98	> 100	NT <sup>b</sup>	> 100	> 100
<b>3</b>	> 100	> 100	> 100	> 100	> 100
<b>4</b>	> 100	> 100	NT	> 100	> 100
<b>5</b>	7.32 ± 1.11	6.09 ± 1.49	> 100	4.61 ± 0.12	56.41 ± 0.47
<b>6</b>	5.85 ± 1.81	8.76 ± 1.21	> 100	7.58 ± 0.13	59.88 ± 1.32
<b>8</b>	> 100	> 100	> 100	> 100	> 100
<b>9</b>	> 100	> 100	> 100	> 100	> 100
<b>10</b>	22.01 ± 0.38	> 100	NT	36.29 ± 1.79	> 100
<b>11</b>	8.20 ± 0.73	11.09 ± 0.98	> 100	13.57 ± 1.09	> 100
<b>13</b>	5.46 ± 1.22	19.28 ± 2.21	NT	11.36 ± 1.02	79.68 ± 1.24
Adriamycin <sup>c</sup>	1.01 ± 0.48	0.72 ± 0.12	1.21 ± 0.63	0.48 ± 0.61	> 100

<sup>a</sup>IC<sub>50</sub>: 50% inhibitory concentration; <sup>b</sup>NT: not tested; <sup>c</sup> Adriamycin: positive control.

per chaperon, arylcarboxylate reductase components, major facilitator superfamily (MFS) transporter, flavin adenine dinucleotide (FAD)-dependent oxygenase, SARP family transcriptional activator, nicotinamide adenine dinucleotide phosphate (NADP) oxidoreductase, and LuxR family transcriptional regulator (Fig. 3A, Table S2).

Previous research has elucidated the synthesis of the phenoxazinone chromophore in compounds 3–7 through a series of enzymatic steps. Initially, dihydroxyacetone phosphate and L-aspartic-4-semialdehyde are catalyzed by PheB and PheC to form 3-amino-4-hydroxybenzoic acid (3,4-AHBA), based on sequence homology with GriI and GriH

from *S. griseus* [20]. PheG and PheH, which are homologous to GriD and GriC, then reduce 3,4-AHBA to 3-amino-4-hydroxybenzaldehyde (3,4-AHBAL) [31]. Finally, PheE and PheF, encoded proteins similar to GriF and GriE, oxidized 3,4-AHBAL to form an *o*-quinone imine derivative. This derivative undergoes a non-enzymatic coupling of two *o*-quinone imine molecules to create the phenoxazinone chromophore (Fig. 3B) [19]. The structural differences among compounds 3–7 primarily involve substitutions at positions C-11 and C-1'. Further examination of the *Phe* gene cluster did not reveal any genes responsible for these specific modifications, suggesting that the genes for these steps may be located out-

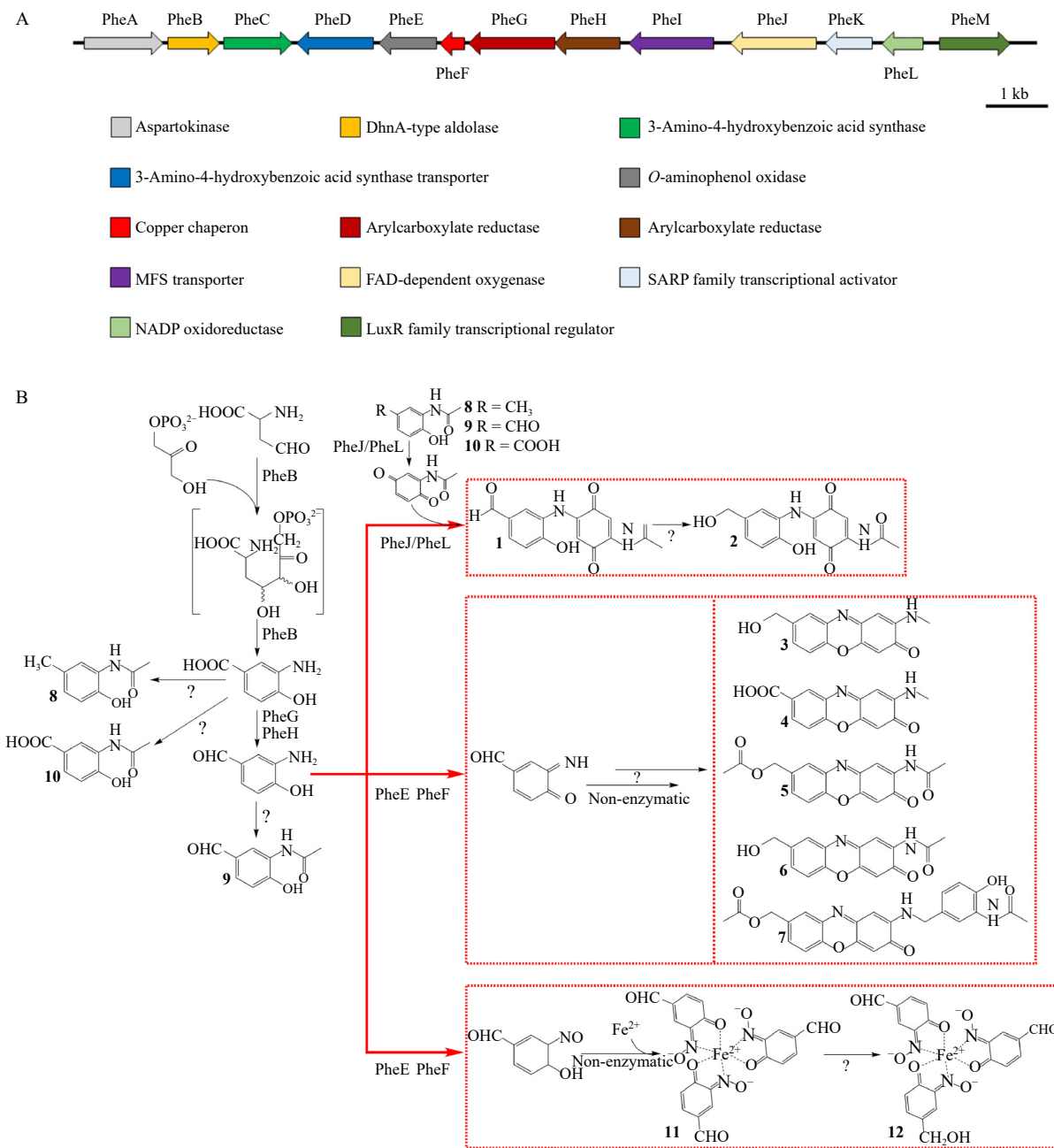


Fig. 3 The *Phe* BGC (A); a proposed biosynthetic pathway for secondary metabolites 1–12 of from *Streptomyces tanashiensis* BYF-112 (B).

side the identified cluster. Additionally, PheE and PhF are similar to NspF and NapE from *Streptomyces murayamaensis*, which catalyze the conversion of 3,4-AHBA to a nitroso derivative. This derivative can non-enzymatically form feroverdin, an analog of viridomycin A (**11**), under ferric ion conditions [29]. It is, therefore, inferred that PheE and PhF might also oxidize 3,4-AHBAL to form a nitroso derivative that subsequently complexes to form viridomycin A (**11**). Viridomycin F (**12**) might be produced by the reduction of one aldehyde group in viridomycin A (**11**) to a hydroxymethylene group by an unidentified reductase.

Compounds **8–10** are considered shunt products in the biosynthetic pathway of *Streptomyces tanashiensis* BYF-112. An arylamine *N*-acetyltransferase, which is not directly involved in the primary biosynthetic pathway, may be responsible for the *N*-acetylation of 3,4-AHBA to produce 3-acetamido-4-hydroxybenzoic acid (**10**) and conversion of 3,4-AHBAL to 3-acetyl-amino-4-hydroxybenzaldehyde (**9**) [32]. The structural difference between *N*-(2-hydroxy-5-methylphenyl)acetamide (**8**) and the other compounds (**9** and **10**) is the presence of a methyl group at C-1. This suggests that *N*-(2-hydroxy-5-methylphenyl)acetamide (**8**) may be produced by an unknown reductase that reduces the carboxyl group of 3,4-AHBA to a methyl group.

Vegfrecine A (**1**) and vegfrecine B (**2**), bearing a unique *p*-benzoquinone ring, are likely derived from the precursor 3,4-AHBA. The quinone skeleton of vegfrecine A (**1**) might be formed by the oxidation of 3,4-AHBA derivatives (compounds **8–10**) catalyzed by the FAD-dependent oxygenase (PheJ) or the NADP oxidoreductase (PheL). The subsequent condensation of 3,4-AHBAL and the *p*-benzoquinone derivative to form vegfrecine A (**1**) could also be catalyzed by these enzymes. The structural difference between vegfrecine A (**1**) and vegfrecine B (**2**) involves the position of the hydroxymethylene group on the benzene ring, suggesting that an unknown reductase might reduce the aldehyde group of vegfrecine A (**1**) to a hydroxymethylene group in vegfrecine B (**2**).

Based on bioinformatic analysis and previous literature, we propose a unique biosynthetic pathway for compounds **1–12**. Notably, three different types of molecules seem to be derived from the same biosynthetic gene cluster (BGC), which contrasts with the conventional view that a single BGC typically produces a single type of metabolite. Moreover, the genes responsible for modifying these metabolites, especially the new compounds (**2**, **3**, and **7**), are not located within the *Phe* BCG. These findings highlight that genome mining strategies for discovering new natural products may overlook unknown compounds present in organisms if only guided by DNA sequences. Further studies are required to elucidate the detailed biosynthetic pathways of compounds **1–12**.

## Experimental

### General experimental procedures

Silica gel (300–400 mesh) for column chromatography

(CC) and silica gel GF<sub>254</sub> for thin layer chromatography (TLC) were sourced from Qingdao Marine Chemical Factory, China. High-resolution electrospray ionization mass spectrometry (HR-ESI-MS) spectra were acquired using a Time-of-Flight Mass Spectrometer G6230AA (Agilent Technologies, Santa Clara, CA, USA). <sup>1</sup>H, <sup>13</sup>C, and 2D nuclear magnetic resonance (NMR) spectra were recorded on an Agilent DD2 600 MHz spectrometer at the Biotechnology Centre of Anhui Agriculture University. Chemical shifts ( $\delta$ ) were referenced to tetramethylsilane (TMS) and solvent signals as internal standards.

### Isolation and identification of BYF-112

*Odontotermes formosanus* specimens were collected from the suburbs of Jiangyin City, Jiangsu Province. Twenty insects were suspended in 1 mL of 1× phosphate buffer, followed by serial dilution to concentrations of 10<sup>-1</sup>, 10<sup>-2</sup>, and 10<sup>-3</sup> in 1× phosphate buffer. From each dilution, 100  $\mu$ L aliquots were plated onto M3 culture medium, which contains 0.12 g of citrate, 0.12 g of citric acid monohydrate, 1.5 g of NaNO<sub>3</sub>, 0.4 g of K<sub>2</sub>HPO<sub>4</sub>·3H<sub>2</sub>O, 0.1 g of MgSO<sub>4</sub>·7H<sub>2</sub>O, 0.05 g of CaCl<sub>2</sub>·H<sub>2</sub>O, 0.02 g of EDTA, 0.2 g of Na<sub>2</sub>CO<sub>3</sub>, and 15.0–20.0 g of agar per liter of sterilized water, supplemented with potassium dichromate (50 mg·L<sup>-1</sup>) and nalidixic acid (25 mg·L<sup>-1</sup>). The plates were incubated at 28 °C for four days to allow bacterial growth. Resulting colonies were sub-cultured on new Gause's No. 1 medium to obtain pure cultures (Fig. S1). The bacterial strain was identified as *Streptomyces tanashiensis* with 99% identity, based on 16S rDNA sequence analysis (GenBank accession number: KU324452.1).

### Cultivation and extraction

*Streptomyces tanashiensis* BYF-112 was initially cultivated in 100 mL of Gause's No.1 medium (20 g soluble starch, 0.5 g KNO<sub>3</sub>, 0.5 g of K<sub>2</sub>HPO<sub>4</sub>·3H<sub>2</sub>O, 0.5 g MgSO<sub>4</sub>·7H<sub>2</sub>O, 0.5 g NaCl, 0.01 g of FeSO<sub>4</sub>·7H<sub>2</sub>O per liter of sterilized water) in a 250 mL flask. After three days of incubation at 28 °C on a rotary shaker at 180 r·min<sup>-1</sup>, 30 mL of the culture was transferred into 400 mL of Gause's No. 1 medium in 1 L flasks (39 × 400 mL, total volume 15.6 L) and incubated at 28 °C on a rotary shaker at 180 r·min<sup>-1</sup> for seven days. The fermentation broth (15.6 L) was then filtered and extracted three times with ethyl acetate (3 × 15.6 L) at room temperature. The combined ethyl acetate extracts were evaporated under reduced pressure to yield a black oily residue.

### Purification of compounds 1–13

The oily residue was subjected to silica gel column chromatography, using dichloromethane/methanol mixtures of increasing polarity (100 : 0, 100 : 1, 100 : 2, 100 : 4, and 100 : 8, *V/V*), resulting in five fractions (Fr. 1–Fr. 5). Fr. 1 ((dichloromethane/methanol 100 : 0, *V/V*) was purified by recrystallization to yield compound **13** (2.8 mg). Fr. 2 (dichloromethane/methanol 100 : 1, *V/V*) was purified by recrystallization to yield compound **8** (10.6 mg). Fr. 3 (dichloromethane/methanol 100 : 2, *V/V*) was separated into four subfractions (R1–R4). Subfraction R1 was further purified by silica gel column chromatography (dichloromethane/

methanol 100 : 8, *V/V*) to yield compounds **11** (8 mg) and **12** (7 mg). Subfraction R2 was recrystallized to yield compounds **5** (18.7 mg) and **10** (13.1 mg). by silica gel column chromatography (petroleum ether/ethyl acetate 10 : 1, *V/V*), followed by Sephadex LH-20 chromatography and recrystallization to yield compound **2**. Fr. 4 (dichloromethane/methanol 100 : 4, *V/V*) was purified by recrystallization to yield compound **9** (10.3 mg) and subfraction R1. Subfraction R1 was further purified by silica gel column chromatography (dichloromethane/methanol mixtures of increasing polarity: 100 : 0, 100 : 1, 100 : 2, 100 : 4, and 100 : 8, *V/V*) to yield four subfractions (R1–R4). R1 was subjected to Sephadex LH-20 column chromatography (methanol) and recrystallized to yield compounds **7** (2.3 mg), **6** (11.7 mg), and **1** (14.6 mg), respectively. Compound **3** (12.3 mg) was purified from subfraction R3 using silica gel column chromatography (petroleum ether/ethyl acetate 10 : 1, *V/V*) and subsequent recrystallization. Subfraction R4 was purified by silica gel column chromatography (dichloromethane/methanol 100 : 4, *V/V*) and recrystallized to yield compound **4** (11.2 mg).

#### Antibacterial bioassay

The antibacterial activity of the metabolites was assessed using the disc diffusion method, as previously described<sup>[11]</sup>. Briefly, *S. aureus*, *M. tetragenus*, and *E. coli* were cultivated on Luria Broth (LB) medium at 37 °C for 12 h. Following this, 0.1% of bacterial suspensions were spread onto solid media plates. Filter paper disks containing 5 µL of metabolite solution (6 mg·mL<sup>-1</sup>) were placed on the plates, which were then incubated at 37 °C for 24 h. The procedure for *P. syringae* pv. *actinidae* was similar, with the exception that the incubation temperature was set at 28 °C.

#### Cytotoxicity bioassay

The cytotoxicity of the compounds was evaluated using the standard colorimetric MTT assay<sup>[33, 34]</sup>. Cells were cultured in DMEM medium containing 10% fetal bovine serum. The cells were then diluted to a concentration of 3 × 10<sup>4</sup> cells/mL in a complete medium, and 100 µL of this suspension was added to each well of 96-well plates. The plates were incubated at 37 °C in a 5% CO<sub>2</sub> atmosphere for 24 h. Various concentrations of compounds (**1–6**, **8–11**, and **13**) were tested against human malignant melanoma cell lines (A375), human ovarian cancer cell lines (SKOV-3), human breast cancer cell lines (MDA-MB-231), human gastric cancer cell lines (MGC-803), and normal cell lines (L02). The IC<sub>50</sub>, representing the concentrations required to achieve 50% inhibition of cell growth, were calculated.

#### Genome sequencing, assembly, and analysis

Genomic DNA from BYF-112 was extracted using a bacterial DNA kit (OMEGA). The genome was sequenced using a combination of PacBio RS and Illumina sequencing platforms. Gene sequences were predicted using Glimmer software version 3.0. De novo assembly was performed using ABySS (<http://www.bcgsc.ca/platform/bioinfo/software/abyss>) and Canu (<https://github.com/marbl/canu>). Sequence annotation was conducted using the non-redundant (NR)

database in NCBI, SwissProt (<http://uniprot.org>), KEGG (<http://www.genome.jp/kegg/>), and COG (<http://www.ncbi.nlm.nih.gov/COG>). Biosynthetic gene clusters (BGCs) for secondary metabolites were identified using antiSMASH v6.0.1.

## Conclusions

In this study, we isolated and identified four new alkaloid derivatives (**1**, **2**, **3**, and **7**) and nine known metabolites (**4–6**, **8–13**) from extracts of *Streptomyces tanashiensis* BYF-112. Among these compounds, viridomycin A (**11**) and viridomycin F (**12**) demonstrated potent antibacterial activities against *Staphylococcus aureus*, *Micrococcus tetragenus*, and *Pseudomonas syringae* pv. *actinidae*. Additionally, viridobruunine A (**5**), exfoliazone (**6**), viridomycin A (**11**), and X-14881E (**13**) exhibited significant cytotoxicity against A375, SKOV-3, and MGC-803 cancer cell lines, with effects comparable to those of adriamycin. The insect-associated *S. tanashiensis* BYF-112 thus represents a promising source of novel antibacterial and anticancer agents. However, further studies are required to elucidate the mechanisms underlying the antibacterial and cytotoxic activities of these compounds. Moreover, our analysis of the BGC responsible for the production of compounds **1–12** revealed that a single BGC could generate three different skeleton types of secondary metabolites. This insight provides a foundation for future bioengineering and biosynthetic research. In conclusion, our investigations offer a theoretical basis for the development of novel bioactive natural products.

## Supporting Information

Supporting information can be requested by sending E-mail to the corresponding author.

## References

- [1] Hug JJ, Bader CD, Remškar M, et al. Concepts and methods to access novel antibiotics from *Actinomycetes* [J]. *J Antibiotics*, 2018, 7: 44.
- [2] Zhang YL, Ge HM, Li F, et al. New phytotoxic metabolites from *Pestalotiopsis* sp. HC02, a fungus residing in *Chondraris roseae* gut [J]. *Chem Biodivers*, 2008, 5: 2402-2407.
- [3] Eggleton P. The state of the world's insects [J]. *Ann Rev Envi and Res*, 2020, 45(1): 61-82.
- [4] Gosalbes MJ, Latorre A, Lamelas A, et al. Genomics of intracellular symbionts in insects [J]. *J Med Microbiol*, 2010, 300: 271-278.
- [5] Van Arnem EB, Ruzzini AC, Sit CS, et al. Selvamycin, an atypical antifungal polyene from two alternative genomic contexts [J]. *Pro Natl Acad Sci USA*, 2016, 113: 12940-12945.
- [6] Zhang AH, Liu W, Jiang N, et al. Sequestration of guest intermediates by dalesconol bioassembly lines in *Daldinia eschscholzii* [J]. *Org Lett*, 2017, 19: 2142-2145.
- [7] Beemelmanns C, Ramadhar TR, Kim KH, et al. Macrotermycins A–D, glycosylated macrolactams from a termite-associated *Amycolatopsis* sp. M39 [J]. *Org Lett*, 2017, 19: 1000-1003.
- [8] Zhang YL, Zhang J, Jiang N, et al. Immunosuppressive polyketides from the mantis-associated *Daldinia eschscholzii* [J]. *J Am Chem Soc*, 2011, 133: 5931-5940.

- [9] Ma SY, Xiao YS, Zhang B, et al. Amycolamycins A and B, two enediyne-derived compounds from a locust-associated *Actinomyces* [J]. *Org Lett*, 2017, **19**(22): 6208-6211.
- [10] Qin ZW, Munnoch JT, Devine R, et al. Formicamycins, antibacterial polyketides produced by *Streptomyces formicae* isolated from African *Tetraponera* plant-ants [J]. *Chem Sci*, 2017, **8**(4): 3218-3227.
- [11] Li S, Shao MW, Lu YH, et al. Phytotoxic and antibacterial metabolites from *Fusarium proliferatum* ZS07 isolated from the gut of long-horned grasshoppers [J]. *J Agr Food Chem*, 2014, **62**: 8997-9001.
- [12] Long YH, Zhang Y, Huang F, et al. Diversity and antimicrobial activities of culturable actinomycetes from *Odontotermes formosanus* (Blattaria: Termitidae) [J]. *BMC Microbiol*, 2022, **22**(1): 80.
- [13] Zhang SX, Wu J, Jiang Z, et al. Pigments of aminophenoxazinones and viridomycins produced by termite-associated *Streptomyces tanashiensis* BYF-112 [J]. *Front. Microbiol*, 2023, **13**: 1110811.
- [14] Nosaka C, Adachi H, Sawa R, et al. Vegfrecine, an inhibitor of vegf receptor tyrosine kinases isolated from the culture broth of *Streptomyces* sp. [J]. *J Nat Prod*, 2013, **76**: 715-719.
- [15] Imai S, Shimazu A, Furihata K, et al. Isolation and structure of a new phenoxazine antibiotic, exfoliazone, produced by *Streptomyces exfoliates* [J]. *J Antibiotics*, 1990, **43**: 1606-1607.
- [16] Gerber NN, Yale HL, Taber WA, et al. Structure and syntheses of texazone, 2-(*N*-methylamino)-3*H*-phenoxazin-3-one-8-carboxylic acid, an *actinomycete* metabolite [J]. *J Antibiotics*, 1983, **36**(6): 688-694.
- [17] Zhang XM, Liu X, Wang Z, et al. ChemInform abstract: viridobrunnines A and B, antimicrobial phenoxazinone alkaloids from a soil associated *Streptomyces* sp. [J]. *Heterocycles*, 2015, **91**(9): 1809-1814.
- [18] Mamedov IG, Eichhoff U, Maharramov AM, et al. Molecular dynamics of *cis*-1-(2-hydroxy-5-methylphenyl) ethanone oxime and *N*-(2-hydroxy-4-methylphenyl) acetamide in solution studied by NMR spectroscopy [J]. *Magn Reson Chem*, 2010, **48**: 671-677.
- [19] Suzuki H, Furusho Y, Higashi T, et al. A novel *o*-aminophenol oxidase responsible for formation of the phenoxazinone chromophore of grixazone [J]. *J Biol Chem*, 2006, **281**: 824-833.
- [20] Suzuki H, Ohnishi Y, Furusho Y, et al. Novel benzene ring biosynthesis from C3 and C4 primary metabolites by two enzymes [J]. *J Biol Chem*, 2006, **281**: 36944-36951.
- [21] Omura S, Enomoto Y, Shinose M, et al. Isolation and structure of a new antibiotic viridomycin F produced by *Streptomyces* sp. K96-0188 [J]. *J Antibiotics*, 1999, **52**(1): 61-64.
- [22] Vanga DG, Kaliappan KP. A unified strategy for the syntheses of angucyclinone antibiotics: total syntheses of tetrangulol, kanglemycin m, X-14881-E, and anhydrolandomycinone [J]. *Eur J Org Chem*, 2012, **11**: 2250-2259.
- [23] Hayakawa Y, Sohda KY, Furihata K, et al. Studies on new antitumor antibiotics, leptofuranins A, B, C and D fermentation, isolation and biological activities [J]. *J Antibiotics*, 1996, **27**: 980-984.
- [24] Kakinuma S, Ikeda H, Takada Y, et al. Production of the new antibiotic tetrahydrokalafungin by transformants of the kalafungin producer *Streptomyces tanashiensis* [J]. *J Antibiotics*, 1995, **48**: 484-487.
- [25] Léo PM, Morin C, Philouze C. Structure revision of medermycin/lactoquinomycin A and of related C-8 glycosylated naphthoquinones [J]. *Org Lett*, 2002, **16**(4): 2711-2714.
- [26] Chung B, Kwon OS, Shin J, et al. Antibacterial activity and mode of action of lactoquinomycin a from *Streptomyces bacillaris* [J]. *Mar Drugs*, 2021, **19**: 7.
- [27] Lu J, He Q, Huang LY, et al. Accumulation of a bioactive benzoisochromanquinone compound kalafungin by a wild type antitumor-medermycin-producing *Streptomyces* Strain [J]. *PLoS One*, 2015, **10**(2): e0117690.
- [28] Guo SQ, Hu HB, Wang W, et al. Production of antibacterial questiomycin A in metabolically engineered *Pseudomonas chlororaphis* HT66 [J]. *J Agric Food Chem*, 2022, **70**(25): 7742-7750.
- [29] Noguchi A, Kitamura T, Onaka H, et al. A copper-containing oxidase catalyzes C-nitrosation in nitrosobenzamide biosynthesis [J]. *Nat Chem Biol*, 2010, **6**(9): 641-643.
- [30] Higashi T, Iwasaki Y, Ohnishi Y, et al. A-factor and phosphate depletion signals are transmitted to the grixazone biosynthesis genes via the pathway-specific transcriptional activator GriR [J]. *J Bacteriol*, 2007, **189**(9): 3515-3524.
- [31] Suzuki H, Ohnishi Y, Horinouchi S. GriC and griD constitute a carboxylic acid reductase involved in grixazone biosynthesis in *Streptomyces griseus* [J]. *J Antibiotics*, 2007, **60**(6): 380-387.
- [32] Suzuki H, Ohnishi Y, Horinouchi S. Arylamine *N*-acetyltransferase responsible for acetylation of 2-aminophenols in *Streptomyces griseus* [J]. *J Bacteriol*, 2007, **189**(5): 2155-2159.
- [33] Wang SB, Liu XH, Li B, et al. Bacteria-assisted selective photothermal therapy for precise tumor inhibition [J]. *J Adv Funct Mater*, 2019, **29**(15): 1-12.
- [34] Chen LZ, Yao L, Jiao MM, et al. Novel resveratrol-based flavonol derivatives: synthesis and anti-inflammatory activity *in vitro* and *in vivo* [J]. *J Eur Med Chem*, 2019, **175**: 114-128.

**Cite this article as:** WU Jun, SONG Tao, ZHANG Le, et al. Antibacterial and cytotoxic metabolites produced by *Streptomyces tanashiensis* BYF-112 isolated from *Odontotermes formosanus* [J]. *Chin J Nat Med*, 2024, **22**(9): 822-830.